

# A Real-Time 32.768-kHz Clock Oscillator Using a 0.0154-mm<sup>2</sup> Micromechanical Resonator Frequency-Setting Element

Henry G. Barrow, Thura Lin Naing, Robert A. Schneider, Tristan O. Rocheleau, Victor Yeh, Zeying Ren, and Clark T.-C. Nguyen  
Dept. of Electrical Engineering and Computer Sciences  
University of California at Berkeley  
Berkeley, CA 94720 USA  
E-mail: [hbarrow@eecs.berkeley.edu](mailto:hbarrow@eecs.berkeley.edu)

**Abstract**— A capacitive-comb transduced micromechanical resonator using aggressive lithography to occupy only 0.0154-mm<sup>2</sup> of die area has been combined via bond-wiring with a custom ASIC sustaining amplifier and a supply voltage of only 1.65V to realize a 32.768-kHz real-time clock oscillator more than 100× smaller by area than miniaturized quartz crystal implementations and at least 4× smaller than other MEMS-based approaches, including those using piezoelectric material. The key to achieving such large reductions in size is the enormous rate at which scaling improves the performance of capacitive-comb transduced folded-beam micromechanical resonators, for which scaling of lateral dimensions by a factor  $S$  provides an  $S^2$ × reduction in both motional resistance and footprint for a given resonance frequency. This is a very strong dependency that raises eyebrows, since the size of the frequency-setting tank element may soon become the most important attribute governing cost in a potential MEMS-based or otherwise batch-fabricated 32.768-kHz timing oscillator market. In addition, unlike quartz counterparts, the size reduction demonstrated here actually reduces power consumption, allowing this oscillator to operate with only 2.1μW of DC power.

**Keywords**—MEMS, micromechanical, resonator, oscillator, real-time clock, 32-kHz clock oscillator.

## I. INTRODUCTION

32-kHz real-time clock oscillators comprise a significant share of the multi-billion dollar oscillator market. Currently, quartz crystal-based oscillators at this frequency dominate the market because they offer the best combination of performance and cost. However, the size of these oscillators is presently too large for future small form factor electronic applications, such as ones that fit within credit card dimensions, including thickness. While attempts have been made to shrink quartz resonating elements [1], the increasingly complex fabrication steps required to produce such devices raises manufacturing costs, thereby preventing widespread adoption (so far). Also, quartz crystal motional resistance values typically increase as resonator dimensions shrink, which in many oscillator configurations raises power consumption [2].

Recent advancements in MEMS technology for frequen-

cy control now offer a vision whereby batch-fabricated MEMS-based oscillators might provide a suitable solution for systems requiring ultra-small components at low cost. Indeed, MEMS-based oscillator companies such as Discera and SiTime have demonstrated commercial success with products (at frequencies higher than 32 kHz) that exhibit adequate drift stability and jitter performance [3]. While 32.769-kHz MEMS-based resonators have recently been released that are 10× smaller than quartz counterparts [4], the potential for even smaller devices remains.

Pursuant to exploring just how small a MEMS-based real-time clock resonator might practically become via sheer scaling, this work uses aggressive lithography to realize a capacitive-comb transduced folded-beam micromechanical resonator that occupies only 0.0154mm<sup>2</sup> of die area, which is more than 100× smaller by area than miniaturized quartz crystal implementations [1] and at least 4× smaller than other MEMS-based approaches, including those using piezoelectric material [5][6]. The combination of this tiny resonator together with a CMOS sustaining amplifier operating in weak inversion provides sustained oscillation with just 2.1μW of DC power consumption and further offers opportunities for significant reductions in power consumption via scaling.

## II. RESONATOR DESIGN

Figure 1 presents a schematic of the overall 32-kHz oscillator, which embeds a capacitive-comb transduced folded-beam micromechanical resonator [7] in a positive feedback loop with a CMOS sustaining amplifier (to be described in more detail, later). The resonator device consists of a 2μm-thick n-doped polysilicon movable shuttle suspended 2μm above an n-doped polysilicon ground plane and connected to its central anchor points via folded beam suspension springs. The overall design essentially mimics the classic design of [7], except that it utilizes interdigitated capacitive-comb finger transducers for not only drive and sense, but also for frequency tuning. In particular, the drive and sense electrodes employ interdigitated fingers that slide

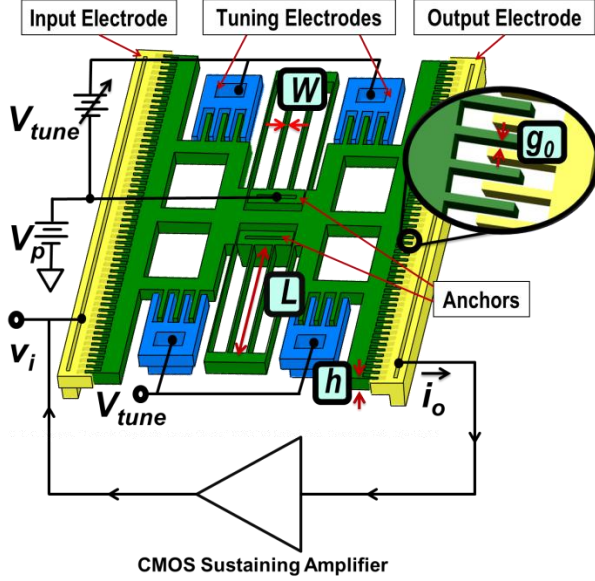


Fig. 1: Perspective-view schematic of the tunable capacitive-comb driven folded-beam resonator connected in a series-resonant oscillator circuit.

relative to one another in a motion that maintains constant gap spacings, which in turn realizes a linear displacement-to-capacitance transfer function that (ideally) eliminates frequency dependence on applied voltages. On the other hand, the fingers of the tuning electrodes move towards or away from one another, in parallel-plate fashion, where their gap spacings mimic shuttle displacements. This generates a nonlinear displacement-to-capacitance transfer function that realizes a voltage-controlled electrical stiffness suitable for frequency tuning [8].

In the hookup of Fig. 1, the sustaining amplifier, together with the applied bias voltages, present a typical two-port bias and excitation scheme for the resonator device. Here, the DC voltage  $V_p$  applied to the resonator shuttle creates an electric field between the shuttle and electrode fingers. An AC (sinusoidal) signal at the device's resonance frequency applied to the input capacitive-comb electrode modulates the electric field across the electrode-to-resonator gap, thereby producing a force that drives the resonator into resonance vibrational motion. This motion in turn modulates the DC-biased capacitance between the vibrating resonator and output electrode fingers, generating an electric current that serves as the device's output.

While this design is already rich in benefits, from the stress-relief afforded by its folded beams, to the frequency stability provided by sliding interdigitated comb-fingers, perhaps its most important benefit is the rate at which reductions in its lateral dimensions decrease its areal footprint and motional resistance.

#### A. Benefits of Scaling

The resonance frequency of the capacitive-comb transduced folded-beam resonator of this work is given by [9]

$$f_0 = \frac{1}{2\pi} \left[ \frac{k_m - k_e}{m_m} \right]^{\frac{1}{2}} = \frac{1}{2\pi} \left[ \frac{2Eh(W/L)^3 - k_e}{m_m} \right]^{\frac{1}{2}} \quad (1)$$

where  $E$  is Young's modulus;  $h$  is thickness;  $W$  and  $L$  are the widths and lengths, respectively, of the beams used in the folded-beam suspension;  $m_m$  is the dynamic mass of the resonator;  $k_m$  is the mechanical stiffness of the folded-beam suspension; and  $k_e$  is the electrical stiffness induced by the parallel-plate tuning electrodes, given by [10]

$$k_e = \frac{V_{tune}^2 \epsilon_0 A_{tune}}{g_{tune}^3} \quad (2)$$

where  $V_{tune}$ ,  $A_{tune}$ , and  $g_{tune}$  represent the potential difference, total combined tuning finger overlap area, and gap spacing, respectively, between the tuning electrode and resonator; and  $\epsilon_0$  is the permittivity of free-space. Equation (1) indicates that when lateral dimensions  $W$  and  $L$  are scaled by the same factor, their ratio  $W/L$  remains fixed, which means the resonance frequency stays the same.

One of the most important factors determining oscillator performance is resonator motional resistance  $R_x$ . For many oscillator configurations, minimizing  $R_x$  not only reduces power consumption, it also raises the power handling ability of the resonator, which in turn can contribute to improved noise performance. For the resonant structure of this work, the motional resistance is given by [9]

$$R_x = \frac{1}{4\pi f_0 Q} \left( \frac{W}{L} \right)^3 \frac{1}{h} \left( \frac{g_0}{N \epsilon_0 V_p} \right)^2 \quad (3)$$

where  $Q$  is the resonator quality factor;  $N$  is the total number of input/output (I/O) comb-fingers on the resonator shuttle; and  $g_0$  is the spacing between them, assumed equal for all finger pairings. As seen in (3), like resonance frequency,  $R_x$  remains constant with constant  $W/L$  scaling. However, if one reduces the gap spacing  $g_0$  in addition to structure lateral dimensions, the motional resistance shrinks very quickly, by a square law.

Of course, device footprint also scales with lateral dimensions. For the resonator design of this work, the die area consumed can be approximated according to

$$Die Area \approx \alpha L^2 \quad (4)$$

where  $\alpha$  is a design-specific scale factor equal to 7.5 for the device of this work. From (3) and (4), when all lateral dimensions (i.e.,  $W$ ,  $L$ , and  $g_0$ ) shrink by scale factor  $S$ , both die area and  $R_x$  decrease dramatically by  $S^2$ . Fig. 2 illustrates this point by plotting both die area and  $R_x$  against lithographic resolution (assumed to set the minimum  $W$  and  $g_0$ ). As shown, the smallest lithographically defined features in this work are 550nm, yielding a motional resistance of  $2M\Omega$  (for a dc-bias  $V_p=1.65V$ ) and a die area of  $0.015mm^2$  ( $\approx 0.12mm \times 0.12mm$ ). The ASML300 Deep-UV stepper employed to achieve these small features actually boasts the capability of attaining features as small as  $0.25\mu m$  in a production environment [11], and if gaps and features this size were possible, they would yield a significantly smaller die area of  $0.0027mm^2$  ( $\approx 0.05mm \times 0.05mm$ ) and an  $R_x$  value of

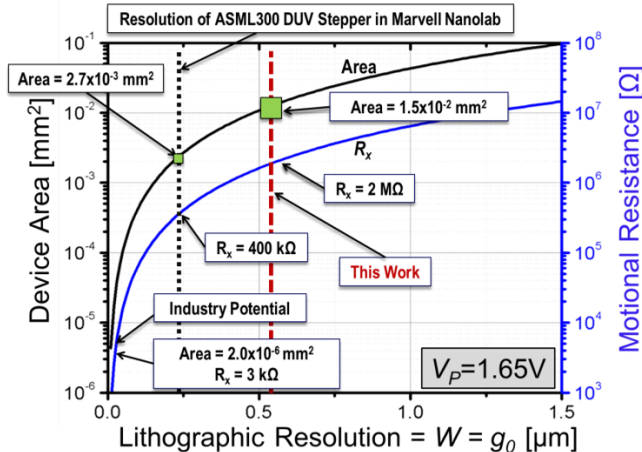


Fig. 2: Plot illustrating the simulated benefits of both motional resistance  $R_x$  and die area when scaling down critical dimensions  $W$  and  $g_0$  as lithographic resolution improves.

only 400k $\Omega$  at the same dc-bias voltage. Ultimately, with the use of 32nm CMOS-grade lithography and patterning techniques already available in industry, and with a (big) assumption that gaps and features this size can be attained in 2 $\mu$ m-thick structural material, this design is theoretically capable of scaling to an extremely small die area of only 0.000002mm<sup>2</sup> ( $\approx 1.4\mu\text{m} \times 1.4\mu\text{m}$ ), while achieving an  $R_x$  of just 3k $\Omega$  with  $V_P=1.65\text{V}$ .

### B. Voltage-Controlled Frequency Tuning

Although the above orders of magnitude improvements in both die area and  $R_x$  as lithographic feature sizes shrink are impressive, concerns naturally arise regarding center frequency variance from device-to-device, especially as features aggressively scale down. To circumvent this problem, the Fig. 1 design employs voltage-controlled frequency tuning, made possible by electrical stiffnesses generated by the parallel-plate transducers previously mentioned.

As illustrated in Fig. 3, this electrical stiffness  $k_e$  arises when the gap  $g_{\text{tune}}$  between a resonator finger and a tuning-electrode finger grows and shrinks. For example, a shrinking gap enhances the electric field generated by the tuning electrode-to-resonator potential difference  $V_{\text{tune}}$ . This varying electric field in turn generates an attractive force that varies in phase with and is proportional to the shuttle displacement—attributes that fit the definition of a negative stiffness. As emphasized in (1), the electrical stiffness  $k_e$ , being negative, counteracts the mechanical stiffness  $k_m$ , resulting in a downward shift in frequency.

Note that because the DC bias voltage  $V_P$  does not appear in (1) or (2), it does not influence the electrical stiffness, so the resonance frequency of the resonator remains unaffected by fluctuations in  $V_P$ . This in turn means that the resonator's motional resistance (given by (3)) and resonance frequency (given by (1)) can be set independently of one another, with the former set by  $V_P$ , and the latter by  $V_{\text{tune}}$ . In other words, the frequency of this device can be adjusted

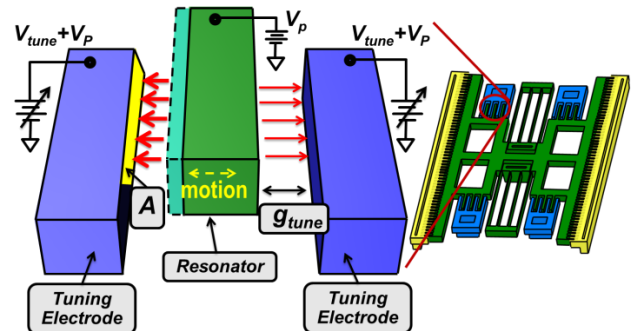


Fig. 3: Perspective-view schematic describing the mechanism behind electrical stiffness generation by the parallel-plate tuning electrodes used to precisely control frequency

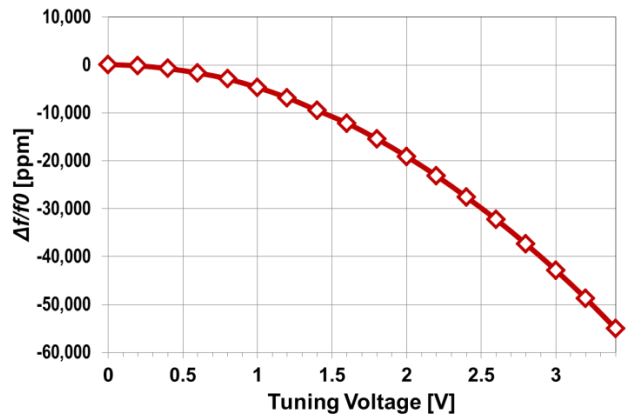


Fig. 4: Measured plot of resonance frequency versus tuning voltage for the device of Fig. 1. Here, the application of 3.3V results in a 50,000 ppm shift in resonance frequency.

without affecting its motional resistance—a very important characteristic for any resonator used in a tunable oscillator.

As observed in (2), in addition to the voltage  $V_{\text{tune}}$ ,  $k_e$  depends on the lithographically designable features  $A_{\text{tune}}$  and  $g_{\text{tune}}$ , meaning the resonator and tuning-electrode designs dictate the overall tuning range. The tuning-electrodes of this work feature 1 $\mu$ m gaps that allow for a 50,000ppm frequency tune over a 3.3V tuning voltage range, as shown by the measured curve of Fig. 4.

### III. RESONATOR FABRICATION

Resonators were fabricated using a conventional 3-mask process flow [7] following the cross-sections shown in Fig. 5. Here, the fabrication steps largely mimic that of previously demonstrated comb-driven resonators, but differ in the use of an ASML300 Deep-UV Stepper for lithography, capable of achieving 0.25 $\mu$ m resolution when operating under ideal conditions [11]. This stepper permits critical features substantially smaller in size than any other published resonator of this type.

Figure 6 presents the scanning electron micrograph (SEM) of a fabricated 32-kHz capacitive-comb driven resonator with 600nm suspension beam widths and 550nm capacitive-comb finger gaps. These diminutive features com-

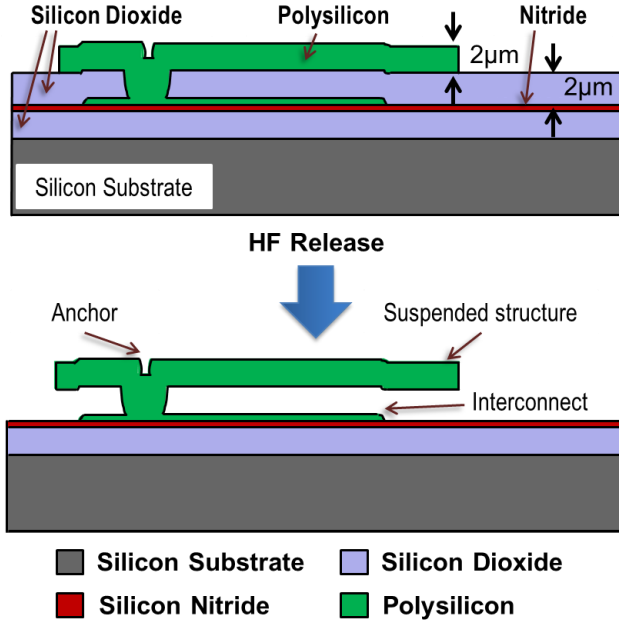


Fig. 5: Cross-sections succinctly illustrating the fabrication process flow used to achieve capacitive-comb driven devices.

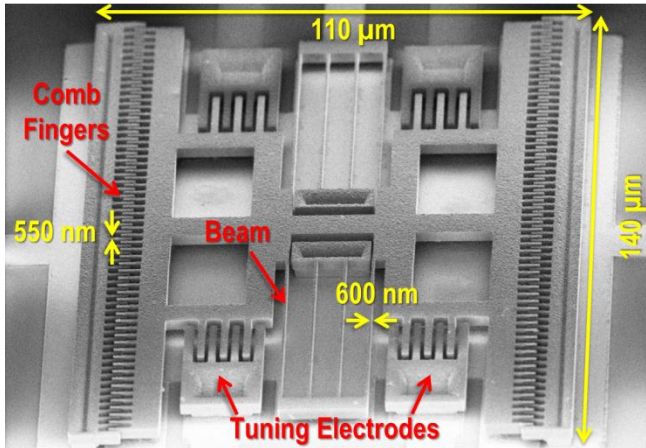


Fig. 6: SEM of a fabricated 32-kHz capacitive-comb driven folded-beam frequency tunable MEMS-based resonator.

bine to deliver a compact device footprint measuring just 110µm×140µm, or 0.0154mm<sup>2</sup>. This compact area is more than 100× smaller than the smallest packaged commercial quartz clock-resonator [1] and at least 4× smaller than the smallest previously demonstrated MEMS-based research resonator [6].

#### IV. CMOS SUSTAINING AMPLIFIER

To attain a clock oscillator, a compatible sustaining amplifier circuit is required. Figure 7 presents the oscillator circuit topology used, here, comprised of a transresistance amplifier in series with the MEMS resonator, represented by an *LCR* tank. When the transresistance gain is 2.8MΩ, this topology yields sufficiently low input and output resistanc-

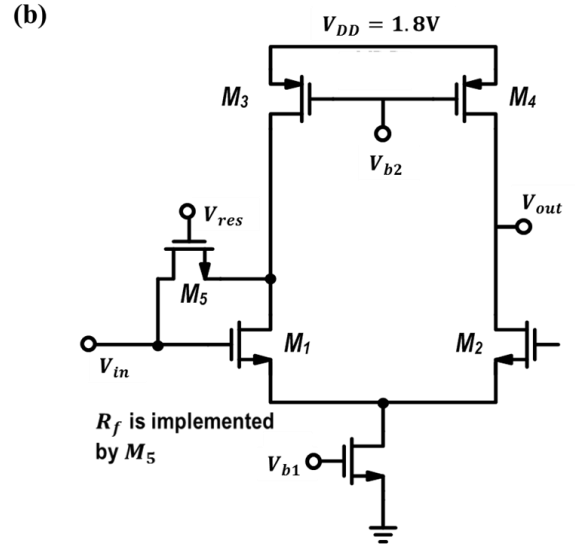
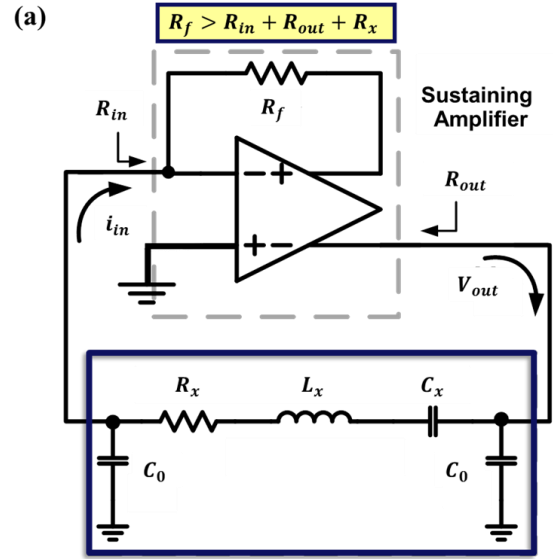


Fig. 7: (a) Top-level circuit schematic of the micromechanical resonator clock oscillator of this work. (b) Transistor level schematic of the custom-designed transresistance sustaining amplifier.

es, on the order of  $R_i=180\text{k}\Omega$  and  $R_o=110\text{k}\Omega$ , respectively, to allow a reasonably small transresistance gain  $R_{amp}$ , where one necessary condition for sustained oscillation requires

$$R_{amp} \geq R_x + R_i + R_o. \quad (5)$$

A second condition for oscillation requires a total 0° phase shift around the oscillator loop. Since the resonator incurs a 0° phase shift across its input/output (I/O) terminals when operating at series resonance, the amplifier must also provide a 0° phase shift from input-to-output.

The circuit of Fig. 7 satisfies the above criteria for sustained oscillation while utilizing a single gain stage designed to minimize common mode noise [12][13]. The sustaining circuit entails a fully balanced differential CMOS op-amp connected in shunt-shunt feedback on one side, with

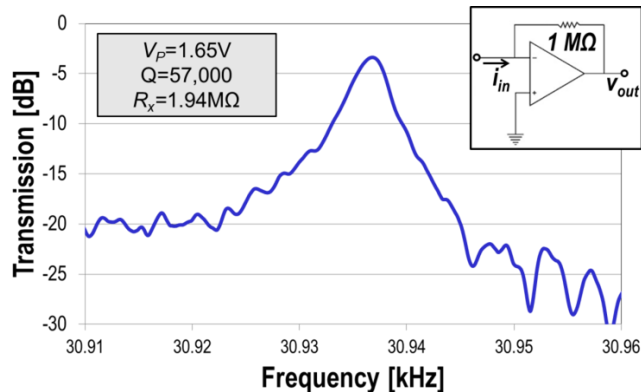


Fig. 8: Measured frequency characteristic for the Fig. 1 device operating under 10 $\mu$ Torr vacuum.

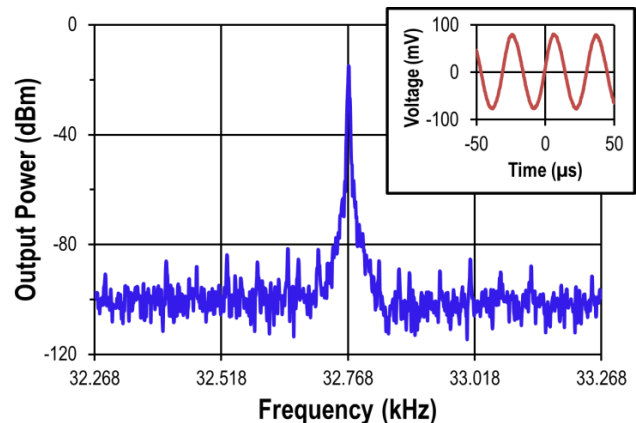


Fig. 10: Measured oscillator output spectrum and time-domain waveform.

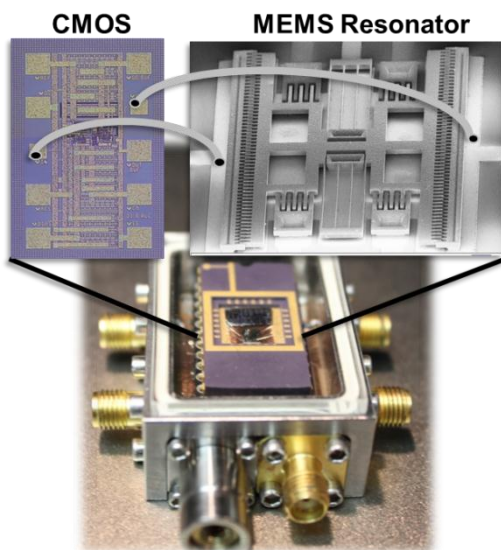


Fig. 9: Photo of the custom vacuum box test apparatus, with a blow up of a mock oscillator schematic combining the SEM of the micromechanical resonator with a die photo of the custom-designed ASIC amplifier.

the output taken from the other side. As detailed in the circuit schematic, the gain stage encompasses transistors  $M_1$ - $M_4$ , while transistor  $M_5$  operates as an MOS resistor to set the large transresistance gain needed to satisfy (5).

## V. EXPERIMENTAL RESULTS

Figure 8 presents the frequency characteristic of the Fig. 1 device operating under 10 $\mu$ Torr pressure in a Lakeshore FWPX Vacuum Probe Station and measured utilizing a 1M $\Omega$  op-amp-based transresistance amplifier into an HP8751A network analyzer. With an applied DC bias voltage of only 1.65V, the resonator exhibited a motional resistance  $R_x$  of 1.94M $\Omega$ , well within the range needed to meet the requirements of the CMOS sustaining amplifier. From (3), it should be noted that while the resonator's high  $Q$  value of 57,000 certainly contributed to the modest  $R_x$  value, the resonator's notably small capacitive-comb gaps  $g_0$  of 550nm were much more responsible for keeping  $R_x$  small.

The custom ASIC CMOS sustaining amplifier of Fig. 7

TABLE I  
OSCILLATOR BIAS AND RESULTS SUMMARY

Resonator Bias $V_p$	1.65V
Supply Voltage $V_{DD}$	1.80V
Tuning Voltage $V_{tune}$	2.95V
Oscillation Amplitude	87.61mV <sub>RMS</sub>
Power Consumption	2.1 $\mu$ W

was fabricated in a 0.35 $\mu$ m foundry process. As depicted in Fig. 9, the oscillator circuit combines the MEMS resonator and sustaining amplifier dies via bond-wires. The oscillator was then placed into a custom-designed vacuum box equipped with feedthroughs for electrical connection to outside measurement instrumentation. Oscillation starts up immediately upon application of the necessary voltages outlined in Table I. As seen in Fig. 10, the oscillator produces a clean sinusoidal time-domain signal with a frequency of precisely 32.768kHz. Note that this exact frequency did not come about via strict process control in fabrication, but rather from application of 2.95V DC to the resonator's tuning-electrodes, which provided the necessary frequency correction. In fact, the measured tuning range of 50,000ppm over a  $V_{tune}$  range of 3.3V is 5 $\times$  greater than the measured device-to-device frequency variance of 10,000ppm, confirming the efficacy of the design described in Section II.

As seen in Table I, sustained oscillation did not call for the application of any voltages above the CMOS technology's design rail of 3.3V. Furthermore, with the transistors forced into weak inversion by lowering the supply-rail to 1.8V, the oscillator consumed only 2.1 $\mu$ W of power, which is on par with the power consumptions of nearly all commercially available compact-footprint clock oscillators.

The clock oscillator of this work compares favorably to previously demonstrated clock oscillators in terms of both size and power consumption Table II and Fig. 11 compare the oscillator and resonator of this work with previously demonstrated 32-kHz oscillators and resonators, respectively. The size comparison illustrated in Table II references all MEMS-die footprints to the package size of the smallest

TABLE II  
OSCILLATOR COMPARISON

Device	SG-3050 [14]	Cioffi & Hsu [5]	Serrano et. al [6]	This Work
Type	Quartz	Capacitive MEMS	Piezoelectric MEMS	Capacitive MEMS
Area	2000μm × 1400μm	~500μm × 400μm	250μm × 250μm	140μm × 110μm
Scale Factor	1	14	44.8	181
V <sub>p</sub>	N/A	2.5V	N/A	1.65V
Q	N/A	60,000	5,000	57,000
Tuning Range	N/A	N/A	6,500ppm over 6V	50,000ppm over 3.3V
Power	2.4μW	1.0μW	N/A	2.1μW

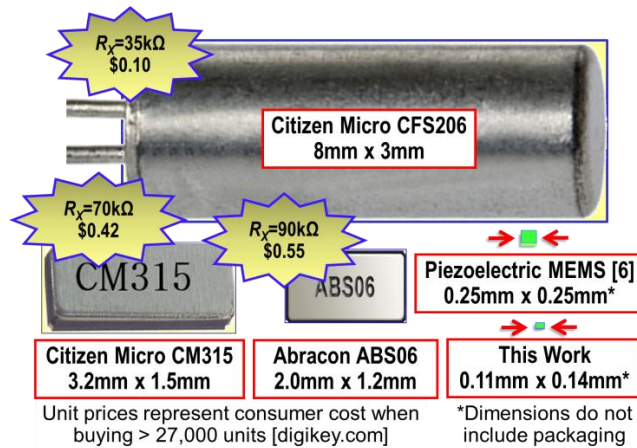


Fig. 11: Size comparison of the resonating element of this work against previously demonstrated miniature clock resonators

commercially available quartz clock oscillator [14], where the larger the scale factor, the smaller the die footprint. From Table II, it can be seen that the oscillator of this work is 181× smaller than its quartz-crystal counterpart and significantly smaller than previously demonstrated MEMS approaches [5][6]. The device of this work also offers a considerably larger tuning range than the recently demonstrated piezoelectric based approach [6], and consumes less power than the smallest commercially available 32-kHz quartz-based product. Given the favorable scaling attributes for capacitive-transduced resonators, highlighted in Section II, even more reductions in size and power consumption should be possible as better lithography becomes available.

## VI. CONCLUSIONS

A 32.768-kHz clock oscillator employing an ultra-compact tunable capacitive-comb transduced MEMS-based resonator as its frequency setting element has been demonstrated with all applied DC-bias voltages < 3V while consuming only 2.1μW of power. The resonator design possesses beneficial scaling properties, whereby scaling-down

all lateral dimensions results in square-law reductions in both motional resistance and die footprint.

Because of this extensive scaling potential, capacitive-transduced MEMS resonators seem well-positioned to provide the smallest real-time clock oscillators provided that the repeatability issues associated with scaling can be mitigated. While the frequency tuning-electrodes in this work provide an effective solution for alleviating center frequency variations exacerbated by aggressive scaling, there is some concern that the large tuning range can give rise to instability if the variables controlling the tuning are themselves not sufficiently stable. For this reason, design improvements that reduce device-to-device mismatch are always desirable and are the subject of future work.

## REFERENCES

- [1] "The World's Smallest SMD 1.6x1.0mm 32.768 Quartz Tuning Fork 'T12'." [Online]. Available: <http://www.txc.com.tw/en/viewproducts/newproden.asp?View=35>.
- [2] J. H. Staudte, "Subminiature Quartz Tuning Fork Resonator," in *27th Annual Symposium on Frequency Control*, 1973, pp. 50 – 54.
- [3] C. S. Lam, "A review of the recent development of MEMS and crystal oscillators and their impacts on the frequency control products industry," in *2008 IEEE Ultrasonics Symposium*, Beijing, China, 2008, pp. 694–704.
- [4] "SiTime Enters \$2 Billion Resonator Market with World's First MEMS Resonator for Real Time Clock and Time Keeping Applications." [Online]. Available: <http://www.sitime.com/news/press-releases/239-sitime-enters-2-billion-resonator-market-with-worlds-first-mems-resonator-for-real-time-clock-and-time-keeping-applications>.
- [5] K. R. Cioffi and W. T. Hsu, "32KHz MEMS-based oscillator for low-power applications," in *Frequency Control Symposium and Exposition. Proceedings of the 2005 IEEE International*, 2005, pp. 551–558.
- [6] D. E. Serrano, R. Tabrizian, and F. Ayazi, "Tunable piezoelectric MEMS resonators for real-time clock," in *Frequency Control and the European Frequency and Time Forum (FCS), 2011 Joint Conference of the IEEE International*, pp. 1–4.
- [7] W. C. Tang, T.-C. H. Nguyen, M. W. Judy, and R. T. Howe, "Electrostatic-comb drive of lateral polysilicon resonators," *Sensors and Actuators*, vol. A21-23, pp. 328-331, 1990.
- [8] K. Wang and C. T.-C. Nguyen, "High-order medium frequency micromechanical electronic filters," *Microelectromechanical Systems, Journal of*, vol. 8, no. 4, pp. 534–556, Dec. 1999.
- [9] C. T.-C. Nguyen and R. T. Howe, "An integrated CMOS micromechanical resonator high-Q oscillator," *Solid-State Circuits, IEEE Journal of*, vol. 34, no. 4, pp. 440–455, Apr. 1999.
- [10] H. C. Nathanson, W. E. Newell, R. A. Wickstrom, and J. Davis, J.R., "The Resonant Gate Transistor," *Electron Devices, IEEE Transactions on*, vol. 14, no. 3, pp. 117 – 133, Mar. 1967.
- [11] "ASML DUV Stepper Model 5500/300." [Online]. Available: <http://nanolab.berkeley.edu/labmanual/chap4/4.19asml300.pdf>.
- [12] Y.-W. Lin, S. Lee, S.-S. Li, Y. Xie, Z. Ren, and C. T.-C. Nguyen, "Series-resonant VHF micromechanical resonator reference oscillators," *Solid-State Circuits, IEEE Journal of*, vol. 39, no. 12, pp. 2477 – 2491, Dec. 2004.
- [13] T. Naing, T. O. Rocheleau, Z. Ren, E. Alon, and C. T.-C. Nguyen, "Vibration-Insensitive 61-MHz Micromechanical Disk Reference Oscillator," in *Frequency Control Symposium and Exposition. Proceedings of the 2012 IEEE International*, 2012, to be published.
- [14] "SG-3050BC Ultra Miniature Size Low Profile Crystal Oscillator." [Online]. Available: <http://www.eea.epson.com/portal/pls/portal/docs/1/1351494.PDF>.